

## Original Article

# Overexpression of miR-31-5p inhibits human chordoma cells proliferation and invasion by targeting the oncogene c-Met through suppression of AKT/PI3K signaling pathway

Wenbo Wang<sup>1,2</sup>, Lejian Tang<sup>1</sup>, Qinghua Li<sup>2</sup>, Jie Tan<sup>2</sup>, Hanxun Yao<sup>1</sup>, Zhengying Duan<sup>1</sup>, Xuewei Xia<sup>1,2</sup>

<sup>1</sup>Department of Neurosurgery, Guilin Medical University, Affiliated Hospital, Guilin, Guangxi, People's Republic of China; <sup>2</sup>Laboratory of Medical Neurobiology, Guilin Medical University, Guilin, Guangxi, People's Republic of China

Received January 20, 2017; Accepted February 23, 2017; Epub July 1, 2017; Published July 15, 2017

**Abstract:** Altered microRNA (miRNAs) expression has been reported in chordoma which has been considered as an important and complex disease. The study aims to explore the mechanism of miR-31-5p in chordoma *in vitro*. We firstly verified miR-31-5p level after mimics transfection using real-time PCR and found over-expressed miR-31-5p could inhibit cell growth and invasive ability, while induce cell apoptosis *in vitro* as detected by CCK8 assay, flow cytometry assay and transwell assay, respectively. Based on prediction result *in silico*, we validated the target gene C-met using dual-luciferase assay and detected the alternation of miR-31-5p as evidence. Using recombinant plasmid, we also found over-expressed c-Met could reduce the effect of over-expressed miR-31-5p on cell growth, cell cycle change, cell apoptosis and invasive ability as detected by CCK8 assay, flow cytometry assay and transwell assay respectively. Meanwhile, it was also appeared that the PI3K/AKT signaling pathway relevant proteins had alternation through WB assays in U-CH1 cells with treatment of miR-31-5p and c-met recombinant plasmid. miR-31-5p may play a protective role in chordoma patients by targeting c-met and then activating PI3K/AKT signaling pathway which suggested that alterations of miR-31-5p might be a useful biomarker and a potential therapy for early detection of chordoma as disease-related molecular and genetic changes.

**Keywords:** miR-31-5p, chordoma, c-Met, PI3K/AKT signaling pathway

## Introduction

As a relatively rare, low-grade mesenchymal tissue tumor, chordoma arises from benign notochordal rests and accounts for 1%-4% of all bone malignancies with an age-adjusted incidence of 0.08/100000 [1, 2]. It has a slow aggressive and locally invasive character predominantly arising at the cranial and caudal ending of the axial skeleton [3]. With histological category of a conventional, de-differentiated and chondroid disease, currently surgical resection is considered to be the most effective therapy for chordoma, since which is reported to be resistant to chemotherapy and radiotherapy relatively [4]. The patients are vulnerable to relapse after surgery with reduced quality of life postoperatively. Little is known about molecular signaling pathways involved in

the chordoma pathogenesis and developing better treatment. Currently, the reliable prognostic markers of chordoma are still under research.

MicroRNAs (miRNAs) are a class of small non-coding single-stranded RNA molecules of about 19-22 nucleotides long, and can regulate gene function including cell proliferation and apoptosis, cell cycle distribution, differentiation and metabolism through translation inhibition or degradation after interacting with 3' UTRs of their target messenger RNA [5, 6]. Previous studies have demonstrated that miRNAs acting as tumor promoters or tumor suppressors are involved in the regulation of several of malignancies. Although reports focusing on miRNAs expression profiling in chordoma are limited, it is reported that miRNA dysregulation correlates

## Potential function of miR-31-5p in human chordoma cells

**Table 1.** Sequence of the primers used for detection of selected miRNA and genes *in vitro*

miRNA	Primers (5'-3')
hsa-miR-31-5p	Forward: ACACTCCAGCTGGGTAGCAGCGGGAACAGTTC
has-miR-31-5p	Reverse: CTCAACTGGTGTCTGTGGA
U6	Forward: CTCGCTTCGGCAGCACA
U6	Reverse: AACGCTTCACGAATTTGCCGT
c-Met	Forward: CATCTCAGAACGGTTCATGCC
c-Met	Reverse: TGCACAATCAGGCTACTGGG
GAPDH	Forward: CGGAGTCAACGGATTGGTCGTAT
GAPDH	Reverse: AGCCTTCTCCATGGTGGTGAAGAC

with tumorigenesis processes in chordoma, and can serve as tumor suppressors or potential prognosis biomarkers [7-10].

Emerging evidence from recent functional studies on one of the altered miRNAs, miR-31, has demonstrated the aberrantly low level of miR-31 in fresh and frozen tissue samples from chordoma patients [11]. In the current study, we over-expressed miR-31 expression *in vitro* and tried to identify the effect of miR-31 on cell proliferation, cell apoptosis, cell cycle change and the ability of cell invasion by serial analyses. And then we found the potential target gene c-Met through screening *in silico* and validated the association between differentially expressed miR-31-5p and the target gene c-Met. Meanwhile, we further explored the effect of elevated expression level of c-Met on cell proliferation, cell apoptosis, cell cycle change and the ability of cell invasion by serial analyses. Finally we tested the expression of other relevant proteins in chordoma disease with a preliminary research of mechanism of miR-31-5p regulating c-Met through PI3K/AKT signaling pathway.

### Materials and methods

#### Cell lines culture and treatment

Human chordoma cells U-CH1 (American Type Culture Collection (ATCC), Manassas, VA) were cultured in IMDM/RPMI 4:1 (PAA Laboratories, Pasching, Austria) supplemented with 2 mM L-glutamine (PAA), 10% FBS (PAA) and 1% PS (PAA) at 37°C and 5% CO<sub>2</sub>. The medium was changed every two or three days according to the recommended culture condition. All cells were harvested by centrifugation, rinsed with phosphate buffered saline (PBS), and subject-

ed to total protein or RNA extraction.

Before diluting into single cell suspensions and seeding in 12-well plates (1 × 10<sup>5</sup> cells/mL), cells were transfected with NC and miRNA mimics for 24 h, 48 h and 72 h respectively, NC as negative control group.

#### RNA isolation and real-time RT-PCR

Using UNIQ-10 columns and TRIZOL Total RNA Isolation Kit (Sangon, Shanghai, China), one microgram of total RNA was isolated and then used for reverse transcription in a reaction volume of 20 µL using Cloned AMV Reverse Transcriptase (Invitrogen, Carlsbad, CA). We used 2 microliters of cDNA for real time PCR using TaKaRa Ex Taq RT-PCR Version 2.1 kit (TaKaRa, Shiga, Japan).

Gene-specific PCR primers for c-Met and GAPDH are listed in **Table 1**. We selected DNA Engine Opticon 2 Continuous Fluorescence Detection System (Bio-Rad, Hercules, CA, USA) for PCR signal detection with conditions from manufacture instruction. Relative amount of c-Met mRNA was normalized to that of GAPDH mRNA.

Expression of mature miRNAs was determined using the miScript primer assays for specific microRNAs (Qiagen GmbH, Germany), and normalized using the 2<sup>-ΔΔCT</sup> method, using Syber Green real-time PCR. PCR reactions were performed in triplicate using Quantitect Syber Green PCR mix (Qiagen, Hilden, USA). The conditions for RT-PCR were 95°C for 6 minutes and then 50 cycles of 95°C for 10 seconds, 55°C for 10 seconds, and 72°C for 30 seconds. Relative amount of miRNAs was normalized to that of U6. All reactions were run in triplicate. All primers used are listed in **Table 1**.

A melting curve analysis was performed for each of the primer sets used, and each showed a single peak indicating the specificity of each of the primers tested.

#### Prediction of miRNA targets

The predicted target genes of the miR-31-5p were screened by TargetScan (<http://www.tar->

## Potential function of miR-31-5p in human chordoma cells

getscan.org/). Then the Functional Gene Ontology (GO) biological processes terms of the putative targets, along with the KEGG pathway analysis, were performed by DAVID. For each GO score, the *P* value of the function enrichment and *P* value of Benjamin correction were calculated. The role of the MAPK pathway in prostate cancer was analyzed by BioChart and KEGG.

### *Luciferase assay*

Small oligonucleotides specific mutation for c-Met from 412 to 430 (NM\_000245) bases (GATCCGGAAGACCTTCAGAAGGTTCTCAAGAGAAACCTTCTGAAGGTCTTCTCTTTTTGGAAA->GATCCGGAAGACCATCAGAAGGTTCTCAAGAGAAACCTTCTGAAGGTCTTCTCTTTTTACGAAA) were cloned and inserted into PCMV3 vector. Before miR-31-5p and PCMV3-c-Met transfection using Lipofectamine 2000 (Invitrogen, Carlsbad, CA), U-CH1 cells transduction ( $1.0 \times 10^5$  cells/mL) were carried out with 350  $\mu$ L of media in the presence of 8  $\mu$ g/ml of polybrene (Sigma) in triplicates in 24-well plates. U-CH1 cells were incubated for additional 36 h after transfection. Thereafter, luciferase activity was performed using the Dual-Luciferase Assay Kit (Promega, Madison, WI, USA) and a Biotek Synergy 4 Microplate reader (Biotek, Vermont, USA). The Relative Light Units (RLU) was calculated using the ratio of Renilla Luciferase/Firefly luciferase and the final values were normalized against PCMV3-c-Met-MUT group and the normalized values were plotted.

### *Plasmid construction*

The synthetic primers of c-Met are as follows: forward (5'-CGAAAGATAAACCTCT CATAATGA-3') and reverse (5'-ATTAAACTTCTT CTTTG-TGG-3'). The nucleotides 169-1133 of human c-Met cDNA (NM\_000245) was amplified by PCR using Takara LA Taq or Primestart (Takara Bio, Kyoto, Japan) and cloned into the PCMV3 vector (Invitrogen, Carlsbad, CA, USA). All joints in the constructs were confirmed by sequencing (Sangon, Shanghai, China). Recombinant plasmid PCMV3-c-Met was transfected into U-CH1 for 24 h which was pre-treated with miR-31-5p mimics for 24 h.

### *Western blotting analysis*

To evaluate the target gene expression change *in vitro* affected by miR-31-5p, proteins extrac-

tion was resolved on 12.5% SDS polyacrylamide gel (SDS PAGE) resolving gel and a 5% stacking gel. Then proteins were electro-transferred onto nitrocellulose membranes at 140 volts for 40 mins. The membranes were treated with antibodies to human c-Met (1:4000, Santa Cruz Biotechnology, Santa Cruz, CA, USA) and anti-human GAPDH (1:10000, Santa Cruz Biotechnology, Santa Cruz, CA, USA) overnight at 4°C after blocking in 5% nonfat powdered milk for 1 h at room temperature. Before incubating with horseradish peroxidase-conjugated secondary antibody IgG (1:10000, Santa Cruz Biotechnology, Santa Cruz, CA) for 1 h, the blot was washed for three times with 10 mins/time at room temperature. SuperSignal West Pico chemiluminescent substrate (Pierce, Rockford, IL) was used for positive antibody reaction. Membranes were exposed to X-ray film (KODAK) for visualization and scanning of protein bands using Alpha Imager software.

### *Cell proliferation detection*

MiR-31-5p mimics (1  $\mu$ g) were transfected into U-CH1 which were seeded at a density of  $1.0 \times 10^5$  cells/mL in 6-well plates for 24 h, 48 h and 72 h, respectively through Lipofectamine™ 2000 (Invitrogen, US). Then, 100  $\mu$ L CCK8 (Dojindo, Japan) solution was added into each well were incubated for 1 h in the incubator. The absorbance was measured at 450 nm using a microplate reader.

### *Apoptosis and cell cycle analysis*

After plasmid transfection for 24 h, the apoptotic cells were quantified using the Annexin V/PI apoptosis kit (Multiscience, Hangzhou, China). Cell suspension was firstly prepared by enzymatic digestion, and centrifuged. Then cells were resuspended in 195  $\mu$ L Annexin V-FITC binding solution with removal of the supernatant. 5  $\mu$ L Annexin V-FITC was added followed by 10 min incubation at room temperature in the dark. The supernatant was removed again after being centrifuged. Subsequently, cells were resuspended in 190  $\mu$ L Annexin V-FITC binding solution, and added with 10  $\mu$ L PI staining solution, which was immediately followed by flow cytometry. Viable cells were resistant to staining with Annexin V-FITC and PI; cells at early stages of the apoptosis were stained with Annexin V-FITC, but not with PI; necrotic cells and cells at late stages of the

## Potential function of miR-31-5p in human chordoma cells

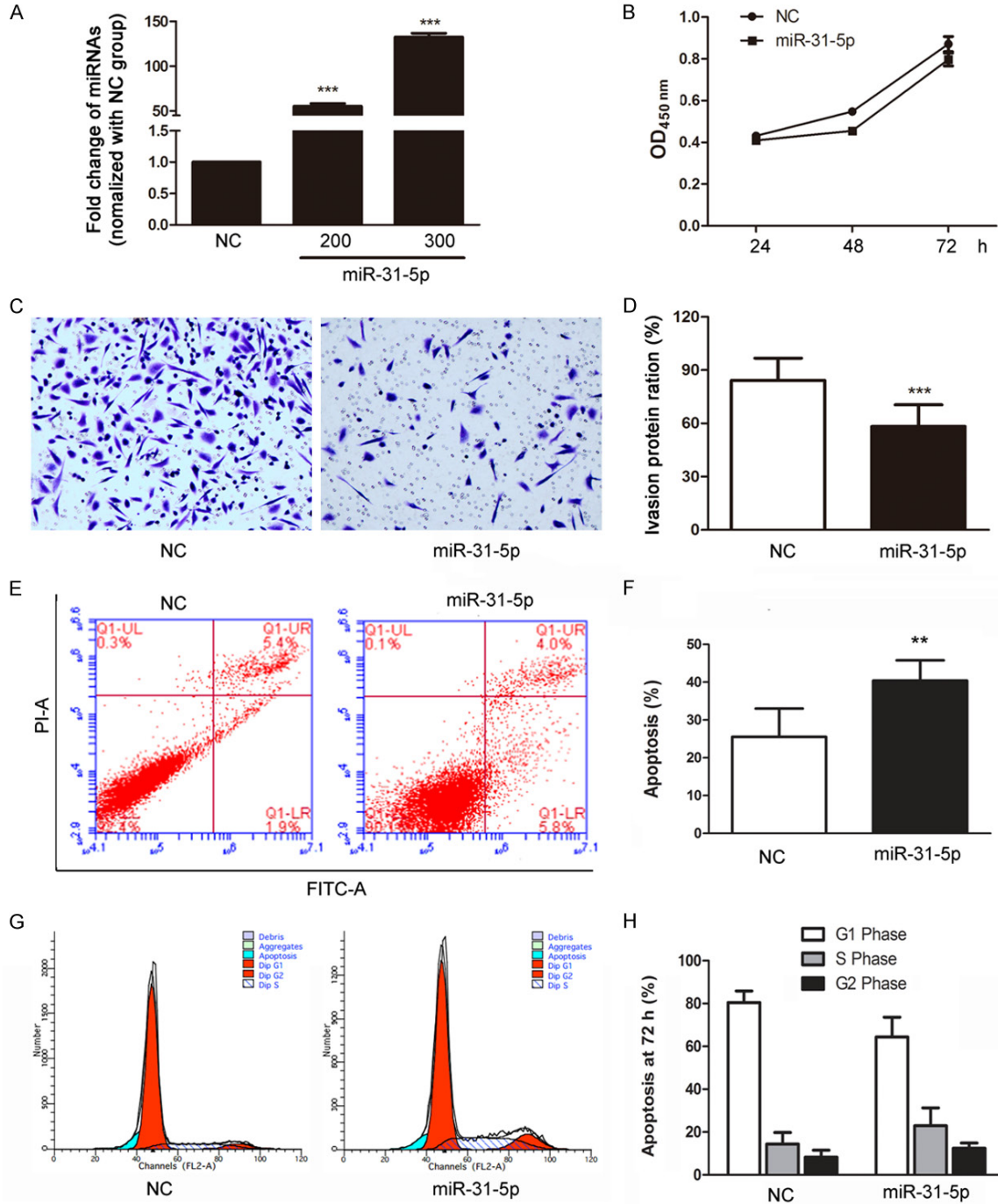


**Figure 1.** Effect of over-expressed miR-31-5p on U-CH1 cell functions. A. Expression of miR-31-5p before mimics transfection as detected by real-time PCR; B. Cell numbers were counted in following time points: 24 hours, 48 hours, 72 hours. Cell viability was measured using CCK8 assay; C, D. Invasive ability tests were performed by transwells inserts without basement membrane extract and the percentage of U-CH1 cells invasive ability in time point of 72 h. U-CH1 cells ( $1 \times 10^5$  cells per well) were seeded in insert with 200  $\mu$ l no-serum medium, 800  $\mu$ l medium containing 5% FBS was added in bottom wells and cells were incubated for 24 hours. Cells were stained with Giemsa; E, F. U-CH1 cells were transfected with mimics for 72 hours before being harvested for apoptosis test and the percentage of U-CH1 cells apoptosis in time point of 72 h; G, H. U-CH1 cells were transfected with mimics for 72 hours before being harvested for cell cycle change detection and the percentage of different phases during cell cycle captured at time point of 72 h. Data are shown as the mean  $\pm$  standard deviation. All experiments were repeated independently three times. \*Indicates  $P < 0.05$ , \*\*Indicates  $P < 0.01$  and \*\*\*Indicates  $P < 0.001$  versus the data from NC group detected at same time point.

## Potential function of miR-31-5p in human chordoma cells

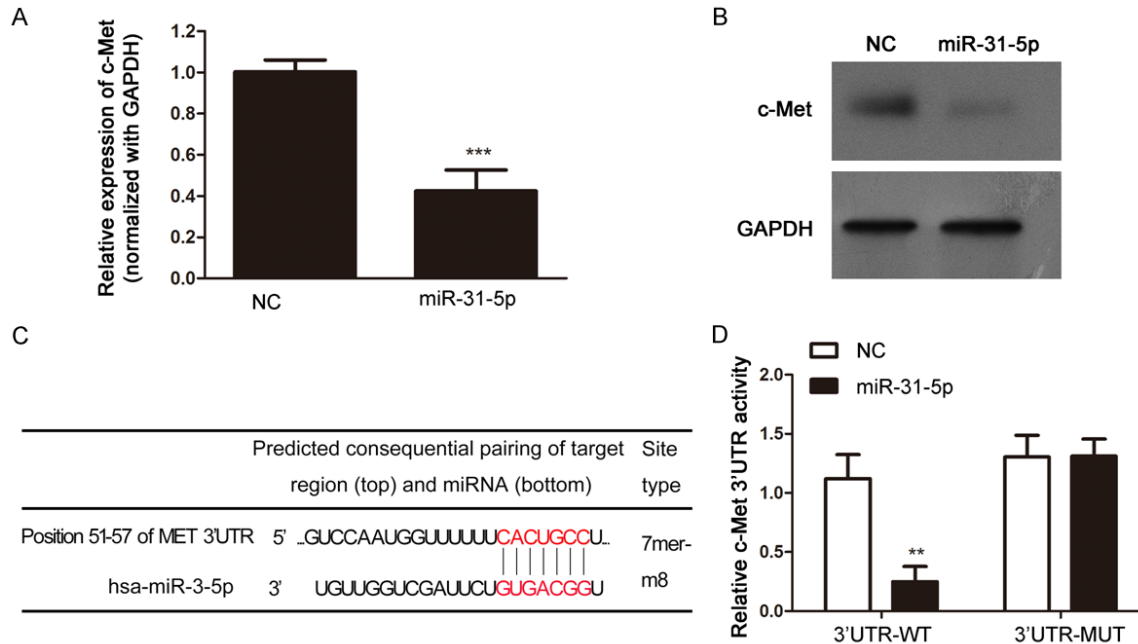


**Figure 2.** Expression of c-Met after miR-31-5p being over-expressed in U-CH1 cells as detected by real-time PCR and western blot analysis. A. mRNA level of c-Met in U-CH1 cells; B. Protein level of c-Met in U-CH1 cells; C. The potential binding region in c-Met; D. miR-31-5p targeted c-Met directly as detected by dual-luciferase assay. All experiments were repeated independently three times. \*Indicates  $P < 0.05$ , \*\*Indicates  $P < 0.01$  and \*\*\*Indicates  $P < 0.001$  versus the data from NC group detected at same time point.

apoptosis were stained with both Annexin V-FITC and PI.

### Transwell assay

After being starved off serum overnight,  $5 \times 10^4$  U-CH1 cells were prepared in serum-free DMEM and seeded into the 24-well transwell upper chambers (8.0  $\mu\text{m}$  pore size; Costar, USA) pre-coated with 100  $\mu\text{g}/\text{ml}$  Matrigel (BD Biosciences) before being inserted into the lower wells containing DMEM with 10% FBS. With incubation for 24 h, the cells remaining on the upper surface of the chamber membrane were removed, and the cells that had invaded to the bottom of the membrane were fixed with methanol and stained with crystal violet. The invaded cells in at least five randomly selected fields at  $200 \times$  magnification were quantified, and images were captured using a phase contrast microscopy equipped with a digital image capturing system.

### Statistical analysis

The data were expressed as mean  $\pm$  SD and analyzed statistically using one-way analysis of variance (ANOVA). Two-way ANOVA was followed

by *post-hoc* Scheffé tests to compare the different treatment groups. Statistical significance was set at  $P < 0.05$ , using SPSS (v 16.0).

## Results

### Effect of over-expressed miR-31-5p on U-CH1 cell functions

The result in **Figure 1A** suggested that miR-31-5p expression was increased dose-dependently after miR-31-5p mimics were treated for 72 h (**Figure 1A**). Then we examined the effects of miR-31-5p on cell proliferation as shown in **Figure 1B**, and found miR-31-5p could inhibit the cell growth in time-independent manner (**Figure 1B**). Furthermore, as shown in **Figure 1C**, the invasion potential of U-CH1 cells of miR-31-5p group was significantly lower than that of the NC group cells (52.26% vs 80.23%,  $P < 0.01$ , **Figure 1D**). Meanwhile we also found that highly expressed miR-31-5p induced U-CH1 cell apoptosis analyzed using flow cytometry after mimics transfection for 72 h based on CCK8 results (**Figure 1E**). U-CH1 cells exposure to mimics presented typical promotion from apoptotic morphology with respect to NC group (**Figure 1F**). Cell cycle distribution

## Potential function of miR-31-5p in human chordoma cells

was analyzed using flow cytometry after mimics transfection for 72 hours. Compared to NC group, Cell cycle testing results showed that ratio of G2/G1 was increased and S cell cycle arrest was increased after mimics transfection (**Figure 1G** and **1H**).

### *Validation of interaction between miR-31-5p and target gene c-Met in vitro*

Based on results of screening *in silico*, we chose c-Met as the candidate of miR-31-5p target gene. Then mRNA level and protein level detection of c-Met were conducted using real-time PCR and western blotting after miR-31-5p mimics transfection. As shown in **Figure 2A** and **2B**, both of mRNA level (**Figure 2A**) and protein level (**Figure 2B**) of c-Met was significantly inhibited in U-CH1 cells after miR-31-5p transfection, compared to NC group at the same time point. To explore the interaction between miR-31-5p and c-Met, cell lysates were detected in dual-luciferase assay system after the potential binding region being predicted *in silico* (**Figure 2C**). With pre-treatment of miR-31-5p mimics, we found PCMV3-c-Met-WT group decreased the luciferase activity in U-CH1 cells (**Figure 2D**), compared to PCMV3-c-Met-MUT group.

### *Effect of over-expressed c-Met on U-CH1 cell functions*

The result in **Figure 3A** and **3B** suggested that c-Met mRNA level (**Figure 3A**) and protein level (**Figure 3B**) were increased after recombinant plasmid transfection for 24 h. Then we examined the effects of c-Met on cell proliferation as shown in **Figure 3C**, and found cellular population was increased time-independently in c-Met over-expressed group especially at 24 h, 48 h and 72 h after recombinant plasmid transfection and miR-31-5p mimics pre-treatment (**Figure 3C**) compared to vector only group. Furthermore, as shown in **Figure 3D** and **3E**, the invasive potential of U-CH1 cells of PCMV3-c-Met group was significantly higher than that of the vector only group cells (43.26% vs 67.23%,  $P < 0.01$ ). Meanwhile we also found that PCMV3-c-Met group inhibited U-CH1 cell apoptosis analyzed using flow cytometry after miR-31-5p mimics transfection for 24 h and PCMV3-c-Met transfection for 48 h following by (**Figure 3F**). U-CH1 cells exposure to mimics and recombinant plasmid presented typical

depression from apoptotic morphology with cell shrinkage, nuclear fragmentation, and cellular rupture into debris. The occurrence of apoptosis was significantly lower in PCMV3-c-Met group with respect to vector only group (**Figure 3G**). Cell cycle distribution was analyzed using flow cytometry after mimics transfection for 72 hours. Compared to NC group, Cell cycle testing results showed that ratio of G2/G1 was decreased and S cell cycle arrest was inhibited after recombinant plasmid transfection (**Figure 3H** and **3I**).

### *miR-31-5p regulate c-Met through PI3K/AKT signaling pathway*

In order to explore the effect of miR-31-5p on chordoma relevant proteins, we harvested U-CH1 cells after miR-31-5p mimics treatment for 24 h and PCMV3-c-Met transfection for 24 h followed by, and then detected c-Met, p-PI3K, PI3K, p-AKT, AKT expression in protein level as **Figure 4** shown. c-Met, p-AKT and p-PI3K expression were down-regulated significantly in U-CH1 cells with overexpressed miR-31-5p which was reversed after miR-31-5p inhibitor transfection. Differently, AKT and PI3K levels in U-CH1 cells didn't show significant change, compared to overexpressed miR-31-5p group (**Figure 4A**). As **Figure 4B** shown, p-AKT and p-PI3K expression were up-regulated significantly in U-CH1 cells with overexpressed miR-31-5p and PCMV-c-Met transfection following by, with respect of PCMV group. Meanwhile, AKT and PI3K levels in U-CH1 cells didn't show significant change.

## Discussion

Currently the main choice of treatment strategy for chordoma is surgical excision, but local recurrence after surgery still exists in around 40% of chordoma patients [12-14]. Through explore of the potential biomarker and therapeutic target of chordoma, previous study found that significantly low expression of miR-31 as a potential novel oncogenic microRNA in chordoma patients but without clear mechanism [11]. To investigate the resolution of this concern, our studies indicated that overexpressed miR-31-5p may decrease cell growth and invasive ability with induced cell apoptosis in U-CH1 cells by directly inhibiting c-Met expression, based on screening results *in silico*. We propose that miR-31-5p has an impor-

## Potential function of miR-31-5p in human chordoma cells

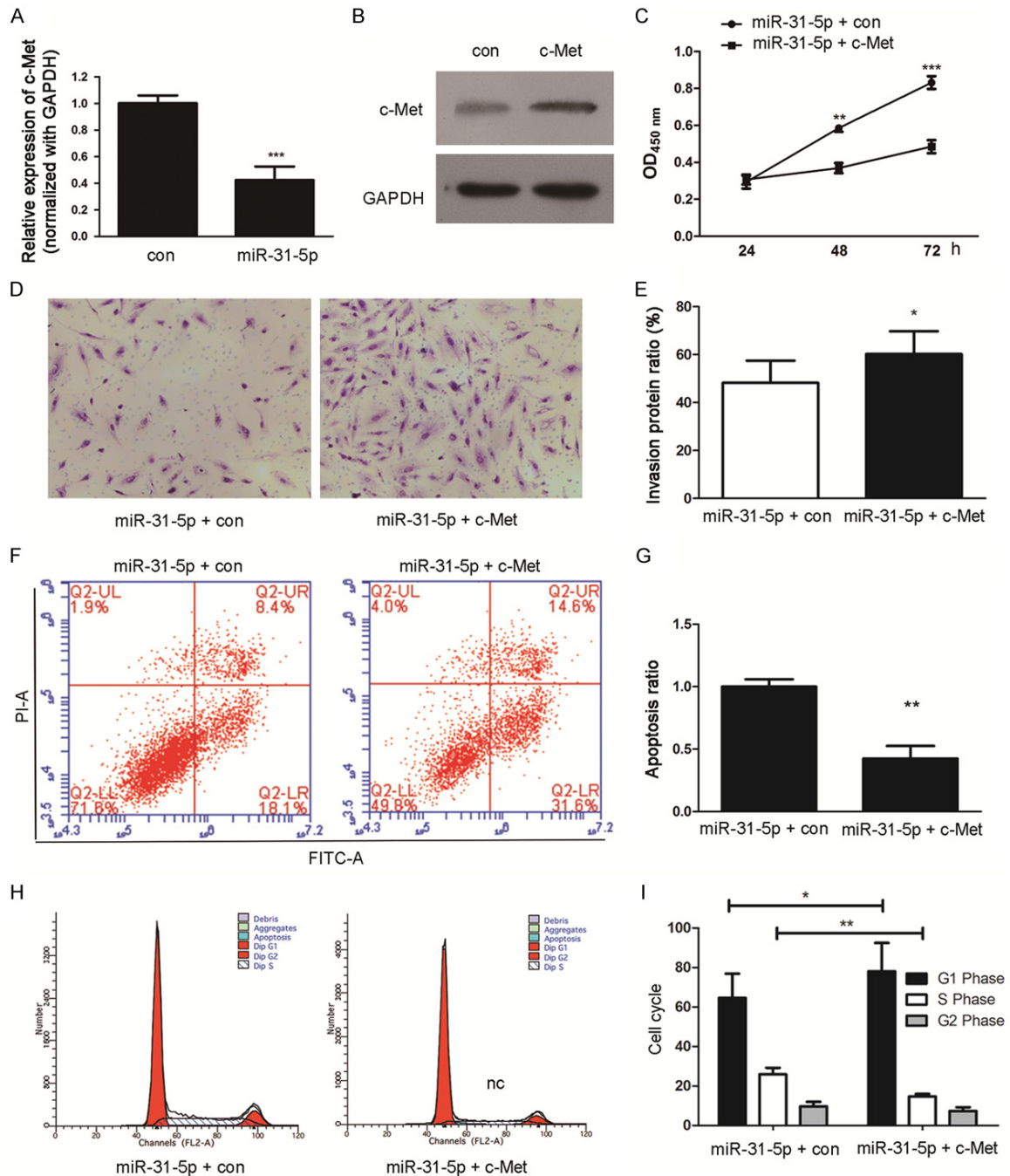


**Figure 3.** Effect of over-expressed c-Met on U-CH1 cell functions after pre-treatment of miR-31-5p. A. mRNA level of c-Met in U-CH1 cells after recombinant plasmid transfection; B. Protein level of c-Met in U-CH1 cells after recombinant plasmid transfection; C. Cell numbers were counted in following time points: 24 hours, 48 hours, 72 hours and 96 hours. Cell viability was measured using CCK8 assay; D, E. Invasive ability tests were performed by transwells inserts without basement membrane extract and the percentage of U-CH1 cells invasive ability in time point of 72 h. U-CH1 cells ( $1 \times 10^5$  cells per well) were seeded in insert with 200  $\mu$ l no-serum medium, 800  $\mu$ l medium containing 5% FBS was added in bottom wells and cells were incubated for 24 hours. Cells were stained with Giemsa; F, G. U-CH1 cells were transfected with miR-31-5p mimics and PCMV3-c-Met following for 72 hours totally before being harvested for apoptosis test and the percentage of U-CH1 cells apoptosis in time point of 72 h; H, I. U-CH1 cells were transfected with miR-31-5p mimics and PCMV3-c-Met following for 72 hours totally before being harvested for cell cycle change detection and the percentage of different phases during cell cycle captured at time point of 72 h. Data are shown as the mean  $\pm$  standard deviation. All experiments were repeated independently three times. \*Indicates  $P < 0.05$ , \*\*Indicates  $P < 0.01$  and \*\*\*Indicates  $P < 0.001$  versus the data from control group detected at same time point. U-CH1 cells treated with miR-31-5p mimics and nc PCMV3 both were considered as the control group.

## Potential function of miR-31-5p in human chordoma cells

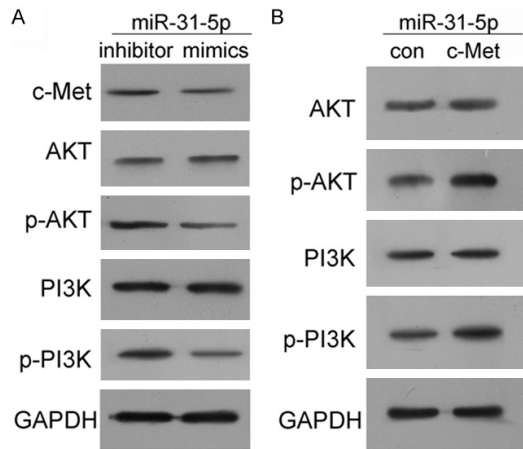


**Figure 4.** miR-31-5p regulate c-Met through activating PI3K/AKT signaling pathway. A. Expression of c-Met, AKT, p-AKT, PI3K, p-PI3K were detected by western blot analysis after mimics/inhibitor transfection respectively; B. Expression of AKT, p-AKT, PI3K, p-PI3K were detected by western blot analysis after mimics/PCMV/PCMV-c-Met transfection respectively. All experiments were repeated independently three times.

tant function as a modulator of c-Met activity in Chordoma. Then our results indicated that miR-31-5p could regulate c-Met by targeting directly as detected by dual-luciferase assay. We tried to over-express the c-Met using transfection of recombinant plasmid after pre-treatment of miR-31-5p mimics and found c-Met reverse the effect of miR-31-5p on cell proliferation, cell apoptosis, cell cycle status and invasive ability. Finally we found the expression of some relevant proteins had alternation. All our results implied that miR-31-5p inhibits c-Met, thereby inhibiting proliferation through the c-Met/PI3K/Akt pathway and activating apoptosis *in vitro*.

C-Met, mainly expressed in epithelial cells, is a transmembrane tyrosine kinase such as Hepatocyte growth factor (HGF) receptor [15]. As a model for a paracrine system in mesenchymal epithelial interaction in many human carcinomas and sarcomas, it is reported that HGF/c-Met signaling system may contribute to tumorigenesis and disease progression or to correlate with invasiveness and poor prognosis [16, 17]. According to previous research, inhibiting c-Met-HGF pair in an HGF+/Met+/PTEN-null glioma model robustly inhibits tumor-initiating capacity, tumor xenograft growth, and resistance to cytotoxic therapeutics [18, 19]. Some other results suggested that PTEN may alter the response of a glioblastoma xenograft mo-

del to HGF/c-Met pathway inhibition through enhancing the inhibition of glioma cell proliferation and tumor angiogenesis but diminishing tumor cell apoptosis [19, 20], which showed that c-Met-HGF plays an important role during tumor prognosis. Scientists also found that c-Met expression was increased in early stage of poorly differentiated tumors like chordoma especially skull base chordoma, which is a unique bone tumor exhibiting a slow growth but an invasive growth pattern, especially in recurrent lesions [21, 22]. C-Met-HGF pair plays a leading role in the formation and metastatic progression in chordoma malignancy. Recent studies also reveal that c-Met may be a potential trigger for the Ras/Map Kinase signaling pathway and PI3K/Akt signaling pathway during tumor prognosis by targeting this receptor tyrosine kinase/ligand system which has anti-oncogenic effects in several pre-clinical model systems [23-25].

### Conclusions

In conclusion, we chose c-Met as the target gene of miR-31-5p based on previous findings and prediction *in silico* and validated our hypothesis using real-time PCR, western blotting and dual-luciferase assay. And then we demonstrated that c-Met affected expression of some relevant proteins through activating PI3K/AKT signaling pathway which implied the underlying mechanism of miR-31-5p's role in chordoma. In the present study, we found that down-regulated miR-31-5p may induce c-Met sensitivity *in vitro*, which may subsequently activate PI3K/AKT signaling pathway as a critical compensatory intracellular event for the survival of U-CH1 cells. Our gene-specific and semiquantitative approaches revealed a potential biomarker with phosphoproteomic data which may provide new insights to clinical application for chordoma disease.

### Acknowledgements

The work is supported by National Natural Science Foundation of China (No. 81560413). Thank the Chordoma foundation for providing U-CH1 cell. Thank Dr. Gary Gallia (Department of Neurosurgery, Johns Hopkins Medical Institutions) for providing technical guidance.

### Disclosure of conflict of interest

None.

## Potential function of miR-31-5p in human chordoma cells

**Address correspondence to:** Dr. Xuewei Xia, Department of Neurosurgery, Guilin Medical University, Affiliated Hospital, Guilin 541001, Guangxi, People's Republic of China. E-mail: xiawxuewei201604@163.com

### References

- [1] Bovbel A, Zaheer A and Maleki Z. Cytomorphologic findings of intraosseous notochordal rest on touch preparation: a case report. *Diagn Cytopathol* 2015; 43: 243-6.
- [2] Shen J, Shi Q, Lu J, Wang DL, Zou TM, Yang HL and Zhu GQ. Histological study of chordoma origin from fetal notochordal cell rests. *Spine* 2013; 38: 2165-70.
- [3] Iorgulescu JB, Laufer I, Hameed M, Boland P, Yamada Y, Lis E and Bilsky M. Benign notochordal cell tumors of the spine: natural history of 8 patients with histologically confirmed lesions. *Neurosurgery* 2013; 73: 411-6.
- [4] Karabagli P, Karabagli H and Yavas G. Aggressive rhabdoid meningioma with osseous, papillary and chordoma-like appearance. *Neuropathology* 2014; 34: 475-83.
- [5] Khan N, Mironov G and Berezovski MV. Direct detection of endogenous MicroRNAs and their post-transcriptional modifications in cancer serum by capillary electrophoresis-mass spectrometry. *Anal Bioanal Chem* 2016; 408: 2891-9.
- [6] Takahashi I, Hama Y, Matsushima M, Hirotani M, Kano T, Hohzen H, Yabe I, Utsumi J and Sasaki H. Identification of plasma microRNAs as a biomarker of sporadic Amyotrophic Lateral Sclerosis. *Mol Brain* 2015; 8: 67.
- [7] Sun X, Hornicek F and Schwab JH. Chordoma: an update on the pathophysiology and molecular mechanisms. *Curr Rev Musculoskelet Med* 2015; 8: 344-52.
- [8] Osaka E, Kelly AD, Spentzos D, Choy E, Yang X, Shen JK, Yang P, Mankin HJ, Hornicek FJ and Duan Z. MicroRNA-155 expression is independently predictive of outcome in chordoma. *Oncotarget* 2015; 6: 9125-39.
- [9] Zou MX, Huang W, Wang XB, Li J, Lv GH, Wang B and Deng YW. Reduced expression of miRNA-1237-3p associated with poor survival of spinal chordoma patients. *Eur Spine J* 2015; 24: 1738-46.
- [10] Zou MX, Huang W, Wang XB, Lv GH, Li J and Deng YW. Identification of miR-140-3p as a marker associated with poor prognosis in spinal chordoma. *Int J Clin Exp Pathol* 2014; 7: 4877-85.
- [11] Bayrak OF, Gulluoglu S, Aydemir E, Ture U, Acar H, Atalay B, Demir Z, Sevil S, Creighton CJ, Ittmann M, Sahin F, Ozen M. MicroRNA expression profiling reveals the potential function of microRNA-31 in chordomas. *J Neurooncol* 2013; 115: 143-51.
- [12] Iacoangeli M, Rienzo AD, Colasanti R, Scarpelli M, Gladi M, Alvaro L, Nocchi N and Scerrati M. A rare case of chordoma and craniopharyngioma treated by an endoscopic endonasal, transtubercular transclival approach. *Turk Neurosurg* 2014; 24: 86-9.
- [13] Zaidi HA, Awad AW and Dickman CA. Complete spondylectomy using orthogonal spinal fixation and combined anterior and posterior approaches for thoracolumbar spinal reconstruction: technical nuances and clinical results. *Clin Spine Surg* 2016; [Epub ahead of print].
- [14] Moojen WA, Vleggeert-Lankamp CL, Krol AD and Dijkstra SP. Long-term results: adjuvant radiotherapy in en bloc resection of sacrococcygeal chordoma is advisable. *Spine* 2011; 36: E656-61.
- [15] Merlin S, Pietronave S, Locarno D, Valente G, Follenzi A and Prat M. Deletion of the ectodomain unleashes the transforming, invasive, and tumorigenic potential of the MET oncogene. *Cancer Sci* 2009; 100: 633-8.
- [16] Park WS, Dong SM, Kim SY, Na EY, Shin MS, Pi JH, Kim BJ, Bae JH, Hong YK, Lee KS, Lee SH, Yoo NJ, Jang JJ, Pack S, Zhuang Z, Schmidt L, Zbar B and Lee JY. Somatic mutations in the kinase domain of the Met/hepatocyte growth factor receptor gene in childhood hepatocellular carcinomas. *Cancer Res* 1999; 59: 307-10.
- [17] Qu Y, Dang S and Hou P. Gene methylation in gastric cancer. *Clin Chim Acta* 2013; 424: 53-65.
- [18] Goodwin CR, Lal B, Ho S, Woodard CL, Zhou X, Taeger A, Xia S and Laterra J. PTEN reconstitution alters glioma responses to c-Met pathway inhibition. *Anticancer Drugs* 2011; 22: 905-12.
- [19] Lal B, Goodwin CR, Sang Y, Foss CA, Cornet K, Muzamil S, Pomper MG, Kim J and Laterra J. *Mol Cancer Ther* 2009; 8: 1751-60.
- [20] Li Y, Guessous F, DiPierro C, Zhang Y, Mudrick T, Fuller L, Johnson E, Marcinkiewicz L, Engelhardt M, Kefas B, Schiff D, Kim J, Abounader R. Interactions between PTEN and the c-Met pathway in glioblastoma and implications for therapy. *Mol Cancer Ther* 2009; 8: 376-85.
- [21] Akhavan-Sigari R, Abili M, Gaab MR, Rohde V, Zafar N, Emami P and Ostertag H. Immunohistochemical expression of receptor tyrosine kinase PDGFR-alpha, c-Met, and EGFR in skull base chordoma. *Neurosurg Rev* 2015; 38: 89-98; discussion 98-89.
- [22] Zhang Y, Schiff D, Park D and Abounader R. MicroRNA-608 and microRNA-34a regulate chordoma malignancy by targeting EGFR, Bcl-xL and MET. *PLoS One* 2014; 9: e91546.

## Potential function of miR-31-5p in human chordoma cells

- [23] Yuen HF, Abramczyk O, Montgomery G, Chan KK, Huang YH, Sasazuki T, Shirasawa S, Gopesh S, Chan KW, Fennell D, Janne P, El-Tanani M and Murray JT. Impact of oncogenic driver mutations on feedback between the PI3K and MEK pathways in cancer cells. *Biosci Rep* 2012; 32: 413-22.
- [24] Holland WS, Chinn DC, Lara PN Jr, Gandara DR and Mack PC. Effects of AKT inhibition on HGF-mediated erlotinib resistance in non-small cell lung cancer cell lines. *J Cancer Res Clin Oncol* 2015; 141: 615-26.
- [25] Byeon HK, Na HJ, Yang YJ, Kwon HJ, Chang JW, Ban MJ, Kim WS, Shin DY, Lee EJ, Koh YW, Yoon JH and Choi EC. c-Met-mediated reactivation of PI3K/AKT signaling contributes to insensitivity of BRAF(V600E) mutant thyroid cancer to BRAF inhibition. *Mol Carcinog* 2016; 55: 1678-87.